

## Chapter 3

### Johnson Noise from Conducting Surfaces [1]

#### 3.1 Introduction to Trap Loss Measurements

As was discussed in Chapter 1, our intuition might suggest that there should be some effect on a trapped cloud of atoms at nano-Kelvin temperatures positioned only tens of microns from a material at 300 K. Obviously, the material will radiate a significant amount of blackbody radiation; however, at room temperature the peak of the blackbody spectra is  $\sim 10 \mu\text{m}$ , thus vanishingly little power is radiated at the primary  $^{87}\text{Rb}$  atomic transition wavelength of  $0.78 \mu\text{m}$ . So, for practical purposes, the atom is unaffected by this blackbody radiation.

Near conducting surfaces, however, there is additional radiation present. In the bulk of a conductor the thermal motion of electrons, commonly referred to as Johnson noise, leads to an additional source of near-field radiation. Henkel *et al.* [16] were the first to predict that this near-field radiation could drive Zeeman spin-flip transitions in magnetically-trapped atoms from trapped to untrapped states. The atoms transferred to untrapped states would then be lost from the trap, therefore the presence of this near-field rf radiation leads to a reduction in the magnetic-trap lifetime.

The first observation of this effect was a microtrap experiment performed by the Hinds group in 2003 [30]. They measured a reduction in their trap lifetime as the trapped atom cloud was brought near a current carrying microtrap wire, and were subsequently able to show that the distance dependence of the loss was not consistent with technical

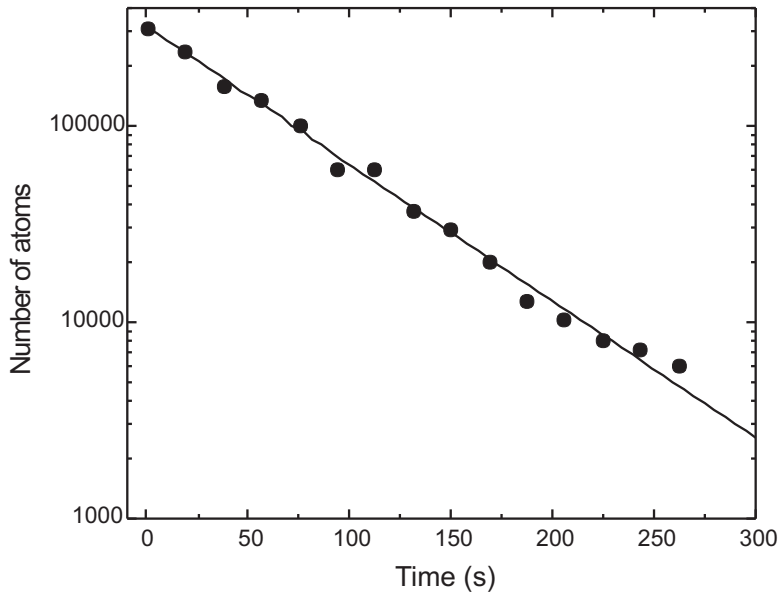


Figure 3.1: Typical data from a lifetime measurement. This lifetime data was taken  $\sim 100 \mu\text{m}$  from the copper surface and at a bias field of 2.57 G.

noise being emitted from the wire. The wire, with a diameter of  $500 \mu\text{m}$ , consisted of a  $370 \mu\text{m}$  diameter copper wire coated with  $55 \mu\text{m}$  of aluminum followed by a  $10 \mu\text{m}$  ceramic layer. Their measurement did clearly illustrate a reduction of trap lifetime near the wire; however, we were interested in making additional measurements because we had the capability to perform the measurement with the flat surface geometry<sup>1</sup> in which the Henkel paper had initially derived the trap loss. Additionally, we had the capability to measure trap loss near materials with different resistivity, allowing a further verification of the theory.

The trap loss measurements were the first atom-surface experiments we undertook, in part because they were quite straightforward. Because our background lifetime was  $\sim 120$  seconds, we expected to see lifetime reductions as far away as  $100 \mu\text{m}$  from the copper surface. This also meant that atom-surface distance uncertainties of several

<sup>1</sup> That is, above a bulk single-material surface, as opposed to the more complicated geometry in the Hinds experiment.

microns would still permit us to make a good measurement. Further, the measurement itself, trap lifetime, is quite easy to perform relative to something like measuring the radial trap frequency to several parts in  $10^5$ , as was necessary for the Casimir-Polder experiment of Chapter 5. All of these factors made this measurement an attractive, and interesting, initial atom-surface experiment to perform.

### 3.2 Experiment

Trap lifetime measurements were made with both normal clouds<sup>2</sup> and condensates. To make a trap lifetime measurement, either a normal cloud at 300-500 nK containing  $\sim 5 \times 10^5$  atoms, or a condensate containing  $\sim 4 \times 10^4$  atoms with a negligible normal component, is prepared in a trap with a bias field  $B_0$  of 3.2 G. Then, over 200-300 ms, the trap center is moved to the desired distance from the surface, and simultaneously the trap bias field is ramped to the desired value, typically 2.57 G, corresponding to a Larmor frequency of 1.80(1) MHz. A low power rf-shield is then turned on  $\sim 400$  kHz above the trap bottom for a normal cloud, or  $\sim 80$  kHz for a condensate, for the duration of the hold time (between 1 ms and 300 s).<sup>3</sup> Finally, the trap center is ramped back to the initial value, and the anti-trapped imaging procedure is performed. A typical lifetime data set is shown in Fig. 3.1.

Most of the components of the apparatus needed to perform this sequence have already been described. The push coils, however, were an older version than was discussed in Section 2.2.7. These push coils, our first version, were each made of three turns of square copper tubing wound onto a phenolic form, see Fig. 3.2. This square tubing is the same tubing that the quadrupole transfer coils are made of. Because they consisted only of three turns, the coils required significantly more current and thus a HP6681A 8 Volt 580 Amp power supply, rather than a battery bank, was used to drive

---

<sup>2</sup> We refer to non-condensed atom clouds as normal clouds.

<sup>3</sup> See Section 2.3.2 for a brief discussion of the rf-shield.

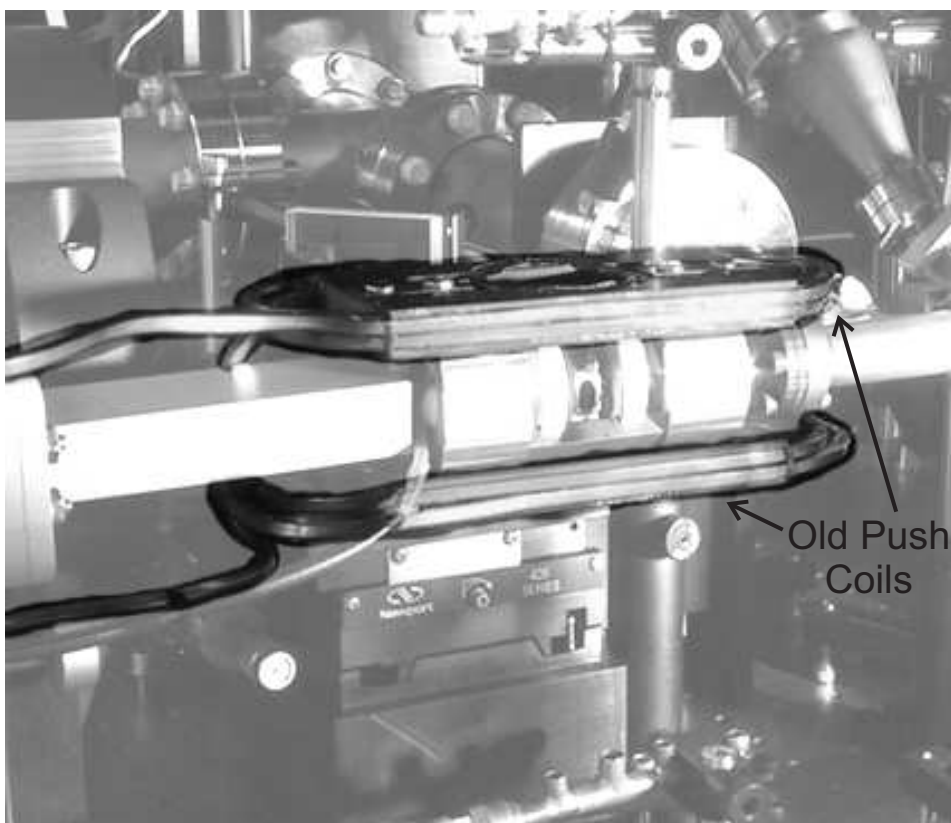


Figure 3.2: An image with the first version of our push coils highlighted.

them.<sup>4</sup> Additionally, because significantly more current was being run through the coils, water cooling of the coils in a manner similar to the quadrupole transfer coils was necessary. The servo system for the current consisted of a single F. W. Bell CLN-300 Hall probe sensor, and a servo circuit similar to the one described in Section 2.2.7.

### 3.3 Results

These measurements were performed using the titanium surface holder, discussed in Section 2.2.1, with three of the different surface materials: copper, titanium, and silicon, with corresponding resistivity of  $1.67(8) \times 10^{-8} \Omega\text{-m}$ ,  $4.88(24) \times 10^{-7} \Omega\text{-m}$ , and  $>1 \Omega\text{-m}$ . Resistivities of copper and titanium were determined by four-wire measurements

<sup>4</sup> This the is the same power supply that drives the quadrupole transfer coils.

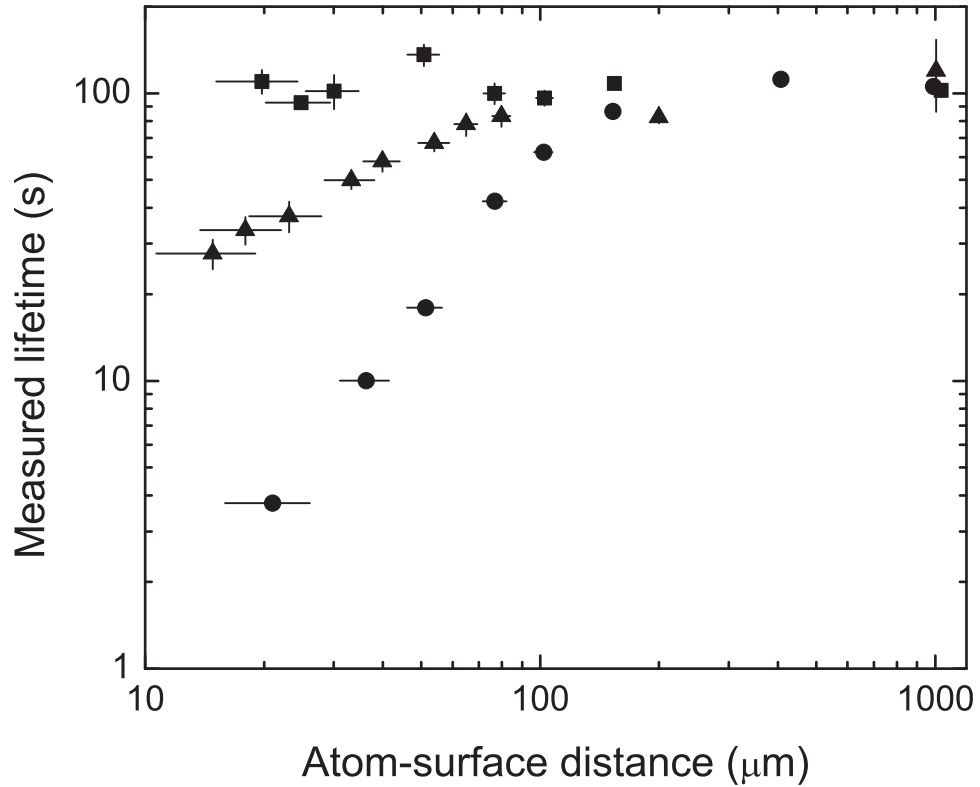


Figure 3.3: Lifetimes of non-condensed (normal) atoms near surfaces of copper (circle), titanium (triangle) and silicon (square);  $\nu_L = 1.80$  MHz for these measurements. The finite width of the atom clouds becomes significant at close distances to the surface, so the radial width of the atom clouds is reflected by the  $x$ -error bars.

using similar samples of copper (99.9999% purity), and titanium (99.7% purity) to those in the vacuum chamber. The measured normal cloud lifetimes as a function of distance to the surface are shown in Fig. 3.3. A number of trends are immediately evident. First, the lifetime near the copper surface drops from the background gas limited rate of  $\sim 120$  s to  $\sim 4$  s in only  $200 \mu\text{m}$ ; this is clearly not a subtle effect. Second, the lifetimes are significantly longer near titanium, which has a resistivity 28 times larger than copper, and near silicon no statistically significant lifetime reduction was observed for atom-surface separations  $>10 \mu\text{m}$ .

For atom-surface separations in the  $100 \mu\text{m}$  range, trap lifetimes near copper and titanium become limited to  $\sim 120$  s due to collisions with the background gas. In order

to examine the trap loss due only to surface effects, the background gas-limited lifetime  $\tau_{BG}$  can be subtracted from the measured lifetime  $\tau_0$  as

$$\tau = \frac{1}{1/\tau_0 - 1/\tau_{BG}}, \quad (3.1)$$

to yield the surface-limited lifetime  $\tau$ . The surface-limited lifetimes for copper, titanium and silicon are shown in Fig. 3.4(a). Additionally, lifetime measurements were made near copper in a trap with a bias field of 8.91 G, corresponding to a Larmor frequency of 6.24(1) MHz, to study Larmor frequency dependence. The surface-limited lifetimes for both 1.80 and 6.24 MHz Larmor frequencies are shown in Fig. 3.4(b).

Theoretical predictions for loss near the surfaces were made following theory derived by Henkel *et al.* [16]. The loss rate from a magnetic trap is

$$\Gamma = \frac{\mu_B^2 g_F^2 \omega_L^2 T}{3\pi\epsilon_0 \hbar^2 c^5} \sum_{\alpha} (h_{\alpha\alpha}(kd) + 1) |\langle f | S_{\alpha} | i \rangle|^2, \quad (3.2)$$

where  $\mu_B$  is the Bohr magneton,  $g_F$  is the Landé  $g$ -factor,  $\omega_L$  is the Larmor frequency ( $\omega_L = \mu_B g_F B / \hbar$ ),  $T$  is the temperature of the surface,  $\epsilon_0$  is the permittivity of free space,  $k$  is the wavenumber ( $k = \omega/c$ ),  $d$  is the distance between the atoms and the surface,  $\alpha$  is the index that sums over  $x$ ,  $y$ , and  $z$  (the coordinate definition is that the  $\hat{z}$ -direction is the direction of the magnetic bias field), and

$$\begin{aligned} h_{xx} = h_{yy} = h_{\parallel}(kd) &= \frac{3}{4} \text{Re} \int_0^{+\infty} \frac{u du}{v} e^{2ivkd} (r_p(u) + (u^2 - 1)r_s(u)), \\ h_{zz} = h_{\perp}(kd) &= \frac{3}{2} \text{Re} \int_0^{+\infty} \frac{u^3 du}{v} e^{2ivkd} r_s(u), \end{aligned} \quad (3.3)$$

$$v = \sqrt{1 - u^2}, \quad (3.4)$$

where the Fresnel coefficients  $r_p$  and  $r_s$  are defined as

$$\begin{aligned}
r_p(u) &= \frac{\varepsilon v - \sqrt{\varepsilon - u^2}}{\varepsilon v + \sqrt{\varepsilon - u^2}}, \\
r_s(u) &= \frac{v - \sqrt{\varepsilon - u^2}}{v + \sqrt{\varepsilon - u^2}}.
\end{aligned} \tag{3.5}$$

Assuming atom loss occurs via the  $|F = 1, m_F = -1\rangle \equiv |i\rangle \rightarrow |F = 1, m_F = 0\rangle \equiv |f\rangle$  transition, following from equation (28) of [16], and using  $S_+$  and  $S_-$  as defined by

$$\begin{aligned}
S_+|F, m_F\rangle &= \sqrt{(F - m_F)(F + m_F + 1)}|F, m_F + 1\rangle \\
S_-|F, m_F\rangle &= \sqrt{(F + m_F)(F - m_F + 1)}|F, m_F - 1\rangle,
\end{aligned} \tag{3.6}$$

allows us write the matrix elements  $\langle f|S_\alpha|i\rangle$  as

$$\begin{aligned}
\langle F = 1, m_F = 0|S_x|F = 1, m_F = -1\rangle &= \frac{\cos\theta}{\sqrt{2}}, \\
\langle F = 1, m_F = 0|S_y|F = 1, m_F = -1\rangle &= -\frac{i}{\sqrt{2}}, \\
\langle F = 1, m_F = 0|S_z|F = 1, m_F = -1\rangle &= -\frac{\sin\theta}{\sqrt{2}},
\end{aligned} \tag{3.7}$$

where  $\theta$  is the angle between the magnetic field and the perpendicular direction to the surface ( $\theta = \pi/2$  in our geometry). Finally, combining 3.2 and 3.7 with  $\theta = \pi/2$  we obtain

$$\Gamma = \frac{\mu_B^2 g_F^2 \omega_L^2 T}{6\pi\varepsilon_0 \hbar^2 c^5} (h_\parallel(kd) + h_\perp(kd) + 2). \tag{3.8}$$

A closed-form asymptotic interpolation of  $h_\parallel(kd)$  and  $h_\perp(kd)$  was estimated in [16] as,

$$\begin{aligned}
h_\parallel(kd) &= \frac{3}{16k^3\delta^2d} \left(1 + \frac{2d^3}{3\delta^3}\right)^{-1}, \\
h_\perp(kd) &= 2h_\parallel(kd),
\end{aligned} \tag{3.9}$$

where  $\delta$ , the skin depth, is defined as

$$\delta = \sqrt{\frac{2\varepsilon_0 c^2 \rho}{\omega_L}}, \quad (3.10)$$

and, finally,  $\rho$  is the resistivity of the surface.

We plot the surface-limited lifetime,  $1/\Gamma$ , using Eq. 3.8 and the interpolation 3.9 in Fig. 3.4(a) as a dotted line. It provides the correct trends, but is not very accurate in the region  $d \sim \delta$ . To more rigorously test the theoretical agreement we additionally calculated the surface-limited lifetime by directly performing numerical integration of Eq. 3.3 to get the solid and dashed theory lines in Fig. 3.4(a) and (b).

We see good agreement between the measured and predicted lifetimes for both the copper at 1.80 and 6.24 MHz Larmor frequencies ( $\delta = 49 \mu\text{m}$  and  $26 \mu\text{m}$  respectively), as well as the titanium at 1.80 MHz Larmor frequency ( $\delta = 262 \mu\text{m}$ ). At the shortest atom-surface distances, the measured lifetimes appear to drop anomalously rapidly. This effect was also seen near silicon, and we suspect that near this length scale the Casimir-Polder force begins to become significant, and can possibly be invoked to explain increased loss.<sup>5</sup> Additionally, at distances within  $10 \mu\text{m}$  of titanium, microwave transitions to the  $|F = 2\rangle$  levels may begin to contribute significantly to the loss as well; this is not accounted for in the plotted theory curves.

The leading systematic effects in this measurement are three-body loss, loss of atoms that tunnel into the surface, and the finite sizes of the atom clouds. Three-body loss, independent of distance to the surface, occurs in normal clouds and condensates, but is much larger in condensates (three-body loss limits condensate lifetimes to  $\sim 40$  s). Due to its lack of dependence of distance to the surface, three-body loss can be removed with  $\tau_{BG}$ . Loss of atoms that strike the surface, or mechanical shaving, is dependent on distance to the surface and the width of the atom cloud. Working with normal clouds and condensates, with typical  $1/e$  and Thomas-Fermi radii of  $4.2 \mu\text{m}$

---

<sup>5</sup> In the May 2003 DAMOP meeting V. Vuletic as well reported seeing loss on an atom chip, he attributed it to Casimir-Polder forces.

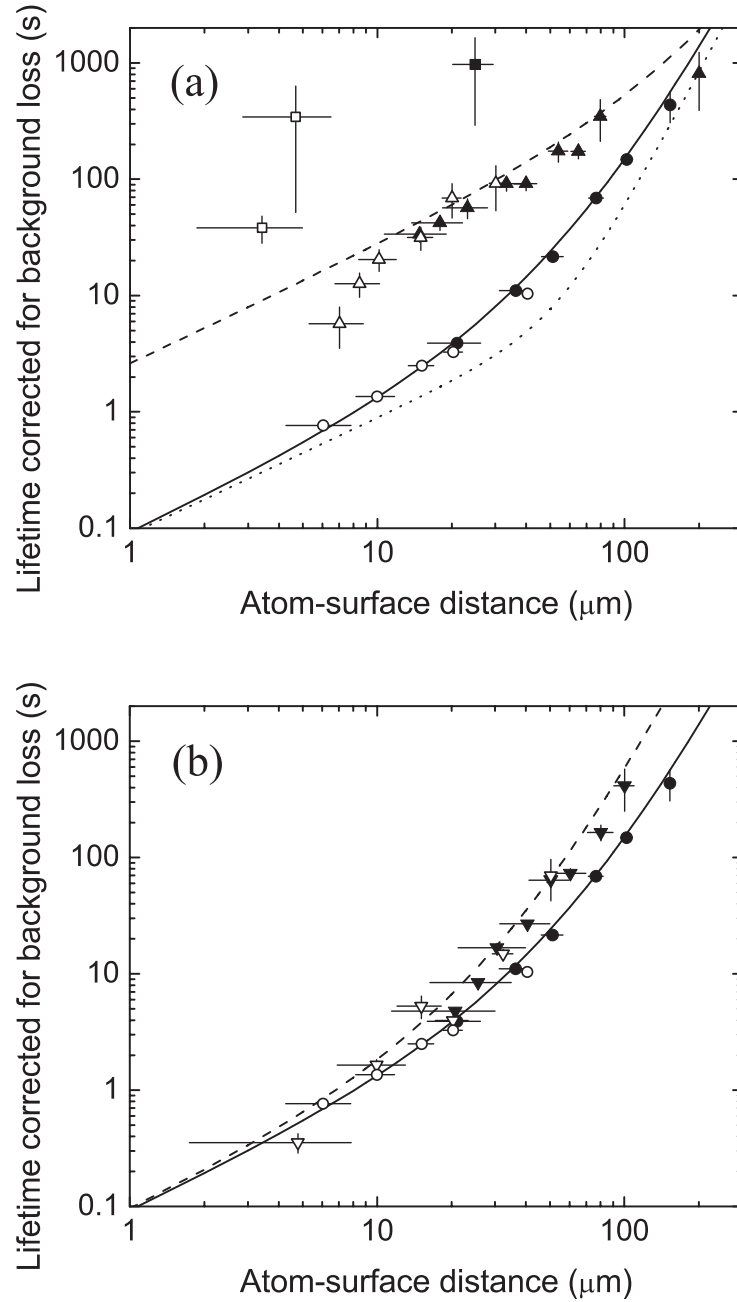


Figure 3.4: Inferred lifetimes near surfaces after subtraction of background loss. (a) Resistivity dependence: copper ( $\bullet$ ), titanium ( $\blacktriangle$ ) and silicon ( $\blacksquare$ ) at  $\nu_L = 1.80$  MHz. Open  $\triangle$  and filled  $\blacktriangle$  symbols represent measurements made with condensates and normal clouds respectively. Solid (Dashed) line indicates lifetimes predicted for copper (titanium). The solid and dashed theory lines are based on a numerical integration of 3.3. The dotted line, plotted for copper, shows the closed-form interpolation 3.9 suggested in [16]. (b) Larmor frequency dependence near copper:  $\nu_L = 1.80$  MHz ( $\bullet$ ) and  $\nu_L = 6.24$  MHz ( $\blacktriangledown$ ). Again, open and filled symbols represent condensate and normal clouds respectively. Solid (Dashed) line indicates lifetimes predicted for  $\nu_L = 1.80$  MHz (6.24 MHz).

and  $1.5 \mu\text{m}$ , respectively, tests for this effect. Good agreement is seen between surface-limited lifetimes measured with condensates and normal clouds, so we feel neither of these systematics is problematic.

There may exist several possible solutions to this problem. The simplest, but possibly the least desirable, is simply to restrict atom-surface separations to separations larger than the skin depth  $\delta$ , which negates some of the advantages that microtraps provide. Second, thin wires, with thickness  $\ll \delta$ , can be used. This significantly can reduce the fluctuating fields generated [30]; however power dissipation becomes increasingly problematic as wires become small. Similarly, wires made from higher resistivity materials can be used, but again power dissipation is a problem. Cooling of the microtrap surface and wires has also been proposed [31]; however for many metals the resistivity scales approximately linearly with temperature, and thus for regions inside the skin depth the lifetime will essentially not improve. In fact, cooling many materials will actually make the trap loss worse. This was highlighted in the recent publication of Dikovskiy *et al.* [32] where the authors note that the important trap loss scaling parameter is  $T/\rho$ , not simply  $T$ . For many pure metals the resistivity  $\rho$  actually decreases faster than linearly with temperature, so the ratio  $T/\rho$  actually increases. In [32] the authors do identify several alloys, such as Ag-Au, that exhibit a decreasing  $T/\rho$  ratio as they are cooled to certain temperatures. Alternatively, this issue may be circumvented by using trapping potentials generated without the use of current-carrying wires; microtraps using permanent magnet structures [34, 33], electrostatic potentials [35], and microoptics [36] have been demonstrated.

### 3.4 Surface Evaporation

We discovered, somewhat accidentally, that the loss of atoms that strike the surface, or mechanical shaving, can be used constructively. By using a surface for position selective removal of atoms, and thus energy selective, one effectively obtains an

evaporation knife [37]. Further, magnetic trap lifetimes near high resistivity materials, such as silicon, are essentially only limited by the background gas collision rate. One could imagine using a high resistivity material as an evaporation knife in the place of rf. Much like rf evaporation, atoms with trajectories that bring them furthest from the trap center, i.e. the most energetic atoms, are removed. Unlike rf evaporation, this evaporation occurs only along one dimension, possibly limiting its efficiency. On the other hand, along this dimension the surface acts as a nearly ideal evaporation surface. As an evaporative knife, the dielectric surface may in effect be “sharper,” removing the high-energy atoms with more certainty, while leaving the low-energy atoms less perturbed than an rf knife.

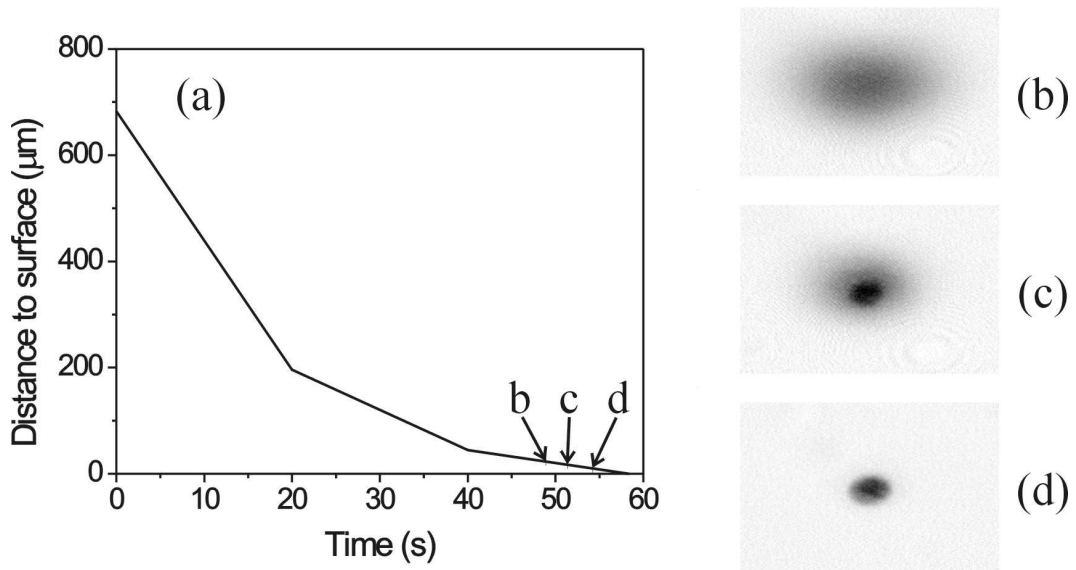


Figure 3.5: Surface evaporation to Bose-condensation: (a) Trap center-surface distance trajectory for silicon surface evaporation. Images showing progressively closer evaporation endpoints and the appearance of the Bose condensate: final atom-surface separations correspond to (b) 23  $\mu\text{m}$  (normal cloud), (c) 17  $\mu\text{m}$  (partially condensed), and (d) 10  $\mu\text{m}$  (nearly pure condensate).

To demonstrate the effectiveness of this technique we load the I-P trap as usual; however we do not apply any rf for evaporation. Instead we apply a series of linear

ramps of the vertical magnetic field, which moves the trap center towards the silicon surface, see Fig. 3.5. The evaporation trajectory is begun with the trap center 700  $\mu\text{m}$  from the surface (our initial temperature is  $\sim 500 \mu\text{K}$ ). Over 50 seconds the trap center is ramped gradually towards the surface, and at a final separation from the trap center to the surface of 10  $\mu\text{m}$  we form a Bose-condensate of  $\sim 5 \times 10^5$  atoms. This is comparable to the size of condensates that can be created through rf evaporation, leading one to conclude that the efficiency of the mechanical evaporation is similar to that of rf evaporation.<sup>6</sup>

Upon initial consideration, it is somewhat surprising that the efficiency of the surface evaporation would be so high because it occurs essentially only in one dimension; however it seems likely that several factors compensate for this. First, the surface is nearly 100% efficient at atom removal – no atoms can pass through the surface and return to the trap center.<sup>7</sup> This means that not only that hot atoms are removed with high efficiency from the trap, but additionally no “Oort” cloud can exist (for example see [25]). Second, the surface is a very “sharp” evaporation surface. With rf evaporation, because of power broadening the rf evaporation knife can either be high power and efficient or low power and narrow, but not both. The surface, on the other hand, is always simultaneously narrow and efficient.

This technique of evaporation may be particularly well suited for continuous condensation schemes [39]. In this case it may be quite difficult to apply spatially varying rf. Instead, by sending the cloud close to a surface, or more specifically having a spatially variable atom-surface separation in an atom guide, evaporation to condensation may be performed “on the fly.”

Unfortunately, for reasons discussed in depth in the next Chapter, a silicon surface

---

<sup>6</sup> The use of surface-induced evaporation to create BEC was also demonstrated by T. Kishimoto, P. Schwindt, Y. J. Wang, and D. Anderson, private communication.

<sup>7</sup> The exception to this is quantum reflection, see [12, 13, 38]. This effect only becomes important for incident velocities of  $\sim 1 \text{ mm/sec}$ .

may not make the optimum evaporation knife. For semi-conducting surfaces,<sup>8</sup> the rubidium atoms that are removed from the trap and end up as adsorbates on the surface generate a significant electric field that in turn distorts the potential near the surface. Thus, if a semiconducting surface were used as a evaporation surface it is likely that its behavior as a evaporation knife would change with time as more atoms adsorb on the surface.

---

<sup>8</sup> This occurs for conducting surfaces as well; however for the reasons described in this Chapter one would likely not choose a conducting surface for the purpose of surface evaporation.